EFFECT OF CALCINATION TEMPERATURE AND DOPING IONS CONCENTRATION ON OPTICAL PROPERTIES OF $YPO_4:Tb^{3+}$

Ngo Quoc Luan[1], Le Thi Thao[2], Nguyen Dang Hoa Nghiêm[2], Chung Dieu Nga[3], and Ngo Khac Khong Minh[2]

[1]Can Tho University
[2]Can Tho University of Technology
[3]Can Tho Technical Economic College
Email: nkkminh@ctuet.edu.vn

ARTICLE INFO
Received: 25/01/2025
Revised: 16/02/2025
Accepted: 18/02/2025

Keywords: *Combustion, emission, luminescence, $YPO_4:Tb^{3+}$*

ABSTRACT

The luminescent nanomaterial $YPO_4:Tb^{3+}$ was successfully synthesized via the combustion method. The crystal structure and optical properties were analyzed using X-ray diffraction (XRD), fluorescence excitation spectroscopy, emission spectroscopy, and lifetime measurements. The synthesized material was single-phase with a tetragonal crystal structure and an average particle size of 20 - 30 nm. Under 220 nm excitation, these materials exhibited a strong blue emission corresponding to the $^5D_4 \rightarrow {}^7F_J$ transitions of Tb^{3+}, with the $^5D_4 \rightarrow {}^7F_5$ transition being the most intense. The optimal synthesis temperature in laboratory conditions was from 800 to 900°C, with the best Tb^{3+} doping concentration at 7 mol%. The measured luminescence lifetime of the material was 363 µs.

1. INTRODUCTION

Nanoscience and nanotechnology are modern interdisciplinary fields that integrate physics, chemistry, and biology. Over the years, both globally and in Vietnam, extensive research has been conducted on nanomaterials in general and luminescent nanomaterials in particular. One of the key advantages of nano-sized luminescent materials is their high uniformity, strong fluorescence intensity, and sharp emission lines (Blasse, 1994; Bhushan, 2004). Rare earth ions play a crucial role in optics due to their strong luminescence, narrow emission bands, long luminescence lifetime, and excellent stability (Hung, 2005). In 2020, Thai Thi Dieu Hien successfully synthesized $GdPO_4:Tb^{3+}$, a material that exhibits blue emission under 273 nm excitation, corresponding to the $^5D_4 \rightarrow {}^7F_J$ transitions of Tb^{3+}, with an optimal doping concentration of 10 mol% (Hien, 2020). Additionally, in 2021, she investigated $YPO_4:Eu^{3+}$ and demonstrated that yttrium orthophosphate is a highly suitable host lattice for rare earth ion doping (Hien, 2021). This suitability arises from its advantageous physical and chemical properties, including a broad optical transparency range, low phonon energy, high quantum efficiency, strong luminescence when combined with an orthophosphate host, excellent thermal and mechanical stability, and environmental friendliness. Furthermore, the Y^{3+} ion has a similar valence state and ionic radius to rare earth dopant ions, facilitating their substitution into the host lattice (Roan, 2009). Due to these advantages, the synthesis and optical characterization of $YPO_4:Tb^{3+}$ have attracted significant research interest. Various synthesis methods have been employed for fabricating $YPO_4:Tb^{3+}$, including hydrothermal synthesis (Ying Yu, 2023), sol-gel processes (Jinyu Yang, 2016), and solid-state reactions

(Weihua Di, 2005). Among these, the combustion synthesis method is particularly promising. This technique relies on an oxidation-reduction reaction between an oxidizing agent, typically nitrate ions (NO_3^-), and a reducing agent, commonly an organic compound containing amino groups ($-NH_2$). The combustion synthesis method offers several advantages, such as the ability to produce large quantities of material, the use of simple equipment, and ease of implementation.

In this study, we synthesized YPO_4:x%Tb^{3+} using the combustion synthesis method and investigated the effects of annealing temperature and dopant concentration on the structural, morphological, and optical properties of the material.

2. EXPERIMENTAL

Materials

The chemicals used for synthesis included Y_2O_3 (Aldrich, 99.99%), Tb_2O_3 (Aldrich, 99.99%), urea (99%, Merck), HNO_3 65% (Merck), H_3PO_4 85% (Merck), and NH_3 25% (Merck).

Synthesis of YPO_4:Tb^{3+}

$Y(NO_3)_3$ (0.2M) and $Tb(NO_3)_3$ (0.02M) solutions were prepared by dissolving Y_2O_3 and Tb_2O_3 in concentrated HNO_3. The required volumes of these solutions, corresponding to the desired dopant concentration (Tb^{3+}), were measured and transferred into a becher. The solution was then evaporated at 70-80°C, with 3 mL of distilled water added after each evaporation cycle. After three evaporation cycles, the resulting metal nitrate mixture was dissolved in 5 mL of distilled water to obtain a homogeneous solution. An appropriate amount of urea was then added, and the solution was stirred at 50°C for 30 minutes to obtain solution 1. A mixture of NH_3 and H_3PO_4 (in a ratio suitable for the target composition) was prepared and stirred at 50°C for 30 minutes, yielding solution 2.

Solution 2 was slowly added to Solution 1 under continuous stirring for 1 hour. The resulting mixture was evaporated and subsequently dried at 80°C for 12 hours, forming a white powder precursor. This precursor was then annealed at temperatures ranging from 300°C to 900°C for 1 hour to obtain the final YPO_4:x%Tb material.

Characterization

X-ray diffraction patterns were recorded using a D8 Advance-Bruker diffractometer at the Faculty of Chemistry, University of Science (Vietnam National University, Hanoi). Fluorescence excitation and emission spectra were measured using a Cary Eclipse spectrofluorometer, equipped with an 80 Hz pulsed xenon lamp as the excitation source. These measurements were conducted at the Institute of Physics, Vietnam Academy of Science and Technology (VAST).

3. RESULTS AND DISCUSSIONS

To study thermal behavior, the precursor sample of YPO_4:5%Tb^{3+} underwent thermal analysis (DTA and TGA) in an air environment from room temperature to 800°C at a heating rate of 10°C/min. The thermal analysis diagram revealed two main mass loss stages within the examined temperature range. The first mass loss occurred between room temperature and 150°C, amounting to 2.9%. This loss was accompanied by an endothermic peak at 91°C, which was attributed to the evaporation of water. The second mass loss took place between 150°C and 350°C, with a significant weight reduction of 55.7%. This stage was associated with two endothermic effects at 226°C and 290°C, likely corresponding to the decomposition of precursor components. Additionally, an

exothermic peak at 316°C was observed, which can be attributed to combustion reactions involving urea and nitrate radicals. Beyond 350°C, the mass loss became negligible, and no further exothermic or endothermic effects were detected. This suggested the formation of the crystalline phase of the material. In the 400-900°C range, the mass remained nearly constant, indicating that the material was thermally stable and no significant chemical reactions occurred in this stage. Based on these thermal analysis results, the temperature range of 300–900°C was selected for further investigation. The obtained samples will be analyzed for structural characteristics using X-ray diffraction (XRD).

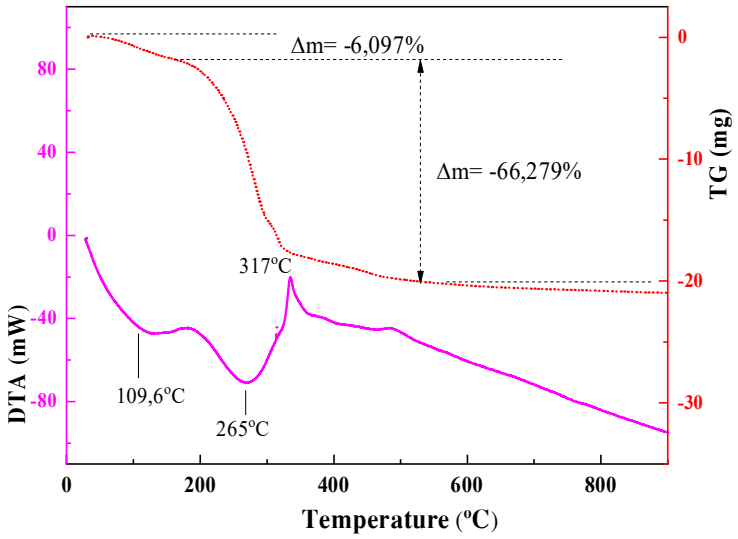

Figure 1. TG/DTA curves of the precursor sample

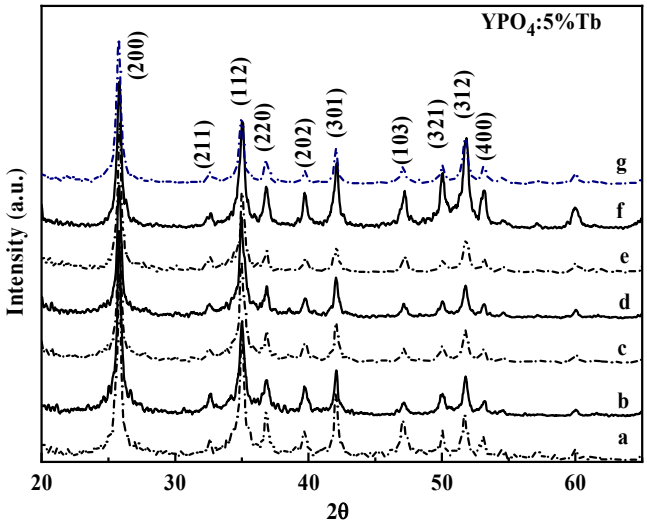

Figure 2. XRD patterns of YPO_4:5%Tb^{3+} material calcined at different temperatures: 300°C(a), 400°C(b), 500°C(c), 600°C(d), 700°C(e), 800°C(f), and 900°C(g)

Figure 2 presents the XRD patterns of YPO_4:5%Tb^{3+} material calcined at different temperatures ranging from 300°C to 900°C for 1 hour. The X-ray diffraction results indicated that the crystalline phase of the YPO_4 matrix was formed when the sample was calcined at 300°C. The synthesized samples exhibited a single-phase tetragonal crystal structure, with all diffraction peaks matching the standard JCPDS 74-2429 card. Several characteristic diffraction peaks appeared at 2θ = 25.8º, 32.5º, 34.9º, 36.7º, 39.6º, 42º, 47.1º, 49.9º, 51.8º, and 53.1º, corresponding to the lattice planes (200), (211), (112), (220), (202), (301), (103), (321), (312), and (400), respectively (Jinyu Yang, 2016). The average crystallite size fell within the range of 21-27 nm. Additionally, while particle aggregation was observed as the calcination temperature increased to 900°C, the extent of this change remains minimal.

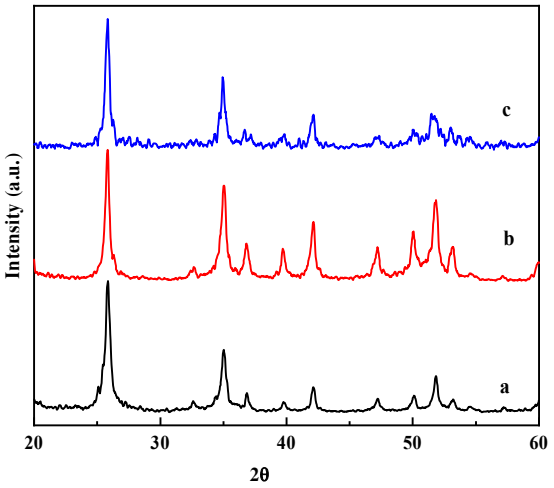

Figure 3. X-ray diffraction patterns of YPO_4:x%Tb^{3+} samples (x=1(a), 5(b), 10(c))

Figure 3 presents the X-ray diffraction (XRD) patterns of YPO_4:x%Tb^{3+} samples (x = 1, 5, 10) calcined at 800°C. The XRD results confirmed the formation of the YPO_4 crystalline phase, indicating that the synthesized material is single-phase with no detectable impurities. All diffraction peaks aligned well with the JCPDS 074-2429 standard card, verifying the material's structural integrity. The average crystallite sizes for the YPO_4:1%Tb^{3+}, YPO_4:5%Tb^{3+}, and YPO_4:10%Tb^{3+} samples were 22 nm, 20 nm, and 21 nm, respectively. These results suggested that varying the Tb^{3+} ion concentration had a negligible effect on grain size and did not induce other phase transitions. Thus, it can be concluded that the synthesis conditions were relatively stable, ensuring reproducibility and structural consistency in the fabricated materials.

The optical properties of the YPO_4:5%Tb^{3+} material were investigated using fluorescence spectroscopy. By analyzing how the optical properties are influenced by doping concentration and annealing temperature, the optimal conditions for material synthesis were evaluated. Figure 4 presents the fluorescence excitation spectrum of YPO_4:5%Tb^{3+} for an emission wavelength of 546 nm. The spectrum had a broad and intense band around 220 nm, which was attributed to the charge transfer band (CTB) between oxygen and Tb^{3+} ions. Additionally, the excitation spectrum exhibited several distinct excitation lines in the 250–300 nm range, corresponding to 4f-5d transitions, as well as direct excitation transitions from the ground state $^7F_6$ to various excited states of Tb^{3+}. Specifically, the excitation line at 317, 340, 350, 368, and 378 nm corresponded to the $^7F_6 \rightarrow {}^5D_0$, $^7F_6 \rightarrow {}^5L_8$, $^7F_6 \rightarrow {}^5L_9$, $^7F_6 \rightarrow {}^5G_6$, and $^7F_6 \rightarrow {}^5D_3$ transitions, respectively (Junfeng Yang, 2018; Hemam Jenee Devi, 2017). These transitions were characteristic of 4f-4f electronic excitations of the Tb^{3+} ion, confirming its incorporation into the YPO_4 host lattice.

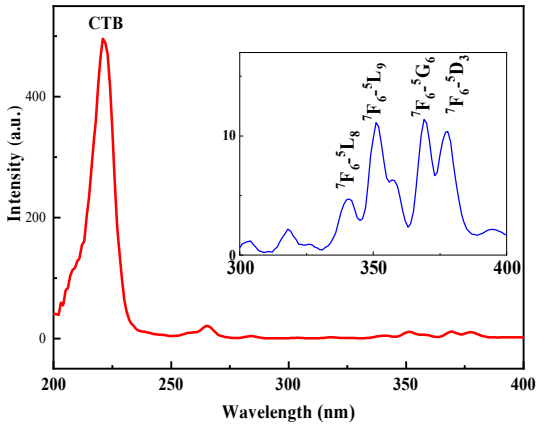

Figure 4. Excitation spectrum of YPO_4:5%Tb^{3+}

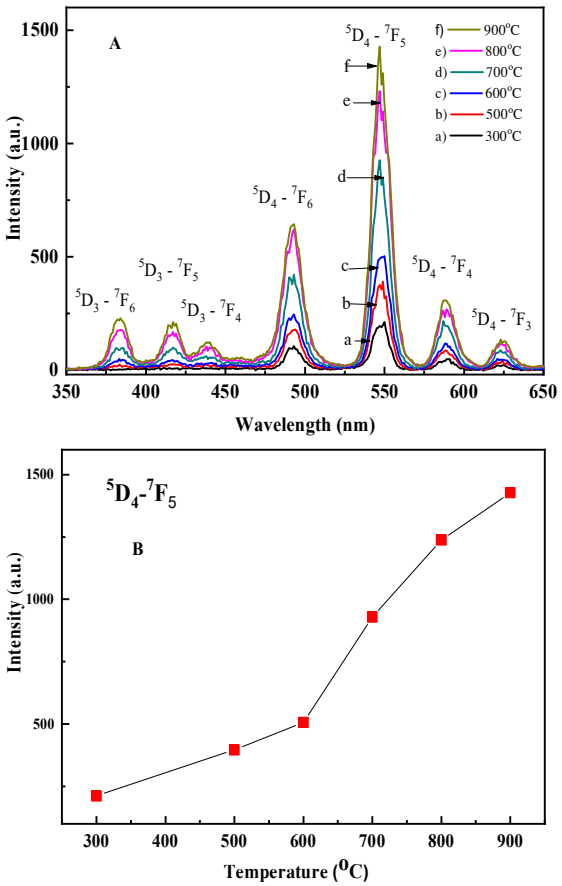

Figure 5. Emission spectra of YPO_4:5%Tb^{3+} samples annealed at different temperatures (A) and the dependence of the intensity of $^5D_4 \rightarrow {}^7F_5$ transition on temperatures (B)

Under excitation at 220 nm, electron transitions within the Tb^{3+} ion occurred. When excited to higher-energy states, the electrons underwent non-radiative relaxation to lower excited states, specifically $^5D_3$ and $^5D_4$, before radiatively transitioning to the ground-state energy levels ^7F_J (J = 3–6), resulting in fluorescence emission. Figure 5 presents the fluorescence spectra of YPO_4:5%Tb^{3+} samples annealed at temperatures ranging from 300°C to 900°C. The spectra exhibited similar shapes across all annealing temperatures, with emission predominantly in the blue region. The fluorescence spectrum consisted of narrow emission lines corresponding to the $^5D_3 \rightarrow {}^7F_J$ and $^5D_4 \rightarrow {}^7F_J$ transitions, specifically: 384 nm ($^5D_3 \rightarrow {}^7F_6$), 417 nm ($^5D_3 \rightarrow {}^7F_5$), 440 nm ($^5D_3 \rightarrow {}^7F_4$), 493 nm ($^5D_4 \rightarrow {}^7F_6$), 546 nm ($^5D_4 \rightarrow {}^7F_5$), 588 nm ($^5D_4 \rightarrow {}^7F_4$), and 623 nm ($^5D_4 \rightarrow {}^7F_3$) (Jinyu Yang, 2016; Wiehua Di, 2005). Among these transitions, the $^5D_4 \rightarrow {}^7F_5$ emission at 546 nm exhibited the highest intensity, making them the dominant feature in the fluorescence spectrum. It is observed that the fluorescence intensity of the $^5D_4$ – $^7F_5$ transition increased as the synthesis temperature rose from 300°C to 900°C. Although X-ray diffraction analysis confirmed the formation of the crystalline phase at 300°C, the fluorescence intensity remained weak at temperatures between 300°C and 600°C. Furthermore, when the synthesis temperature exceeded 800°C, the fluorescence intensity began to approach saturation. The presence of characteristic Tb^{3+} emissions confirmed that these ions were well dispersed within the YPO_4 matrix. Based on these findings, the optimal calcination temperature for YPO_4:Tb^{3+} material in this study was determined to be in the range of 800-900°C.

Figure 6 presents the fluorescence spectra of YPO_4:x%Tb^{3+} (x = 0.1-15)

samples calcined at 800°C under 220 nm excitation. All samples exhibited characteristic emission transitions of Tb^{3+} ions in the YPO_4 matrix. It is observed that the fluorescence intensity varied significantly with increasing Tb^{3+} doping concentration. This was due to the increased number of luminescent centers, which enhanced the overall luminescence intensity. Notably, no fluorescence quenching effect was observed even at a high doping concentration of 15% Tb^{3+}. However, as shown in Figure 6, the fluorescence intensity increased significantly with Tb^{3+} doping concentrations ranging from 0.1% to 7%, but it began to show signs of saturation when the concentration exceeded 7%. Additionally, the $^5D_3 \rightarrow {}^7F_5$ emission was observed in samples with Tb^{3+} concentrations of 0.1%, 1%, 2%, and 3%, but it started to diminish as the concentration increased beyond 5% to 15%. This attenuation can be explained by the following mechanism: At high Tb^{3+} concentrations, the distance between neighboring Tb^{3+} ions decreased, leading to an increased probability of non-radiative energy transfer. This facilitated the cross-relaxation process from $^5D_3 \rightarrow {}^5D_4$, where energy was transferred between neighboring Tb^{3+} ions. As a result, more Tb^{3+} ions accumulated in the $^5D_4$ state, leading to stronger emissions from the $^5D_4 \rightarrow {}^7F_J$ transitions (J = 1, 2, 3, 4, 5, 6). These observations confirmed that increasing the Tb^{3+} concentration enhanced fluorescence intensity, energy transfer mechanisms at higher concentrations favored $^5D_4$-based emissions, leading to reduced $^5D_3$ emissions.

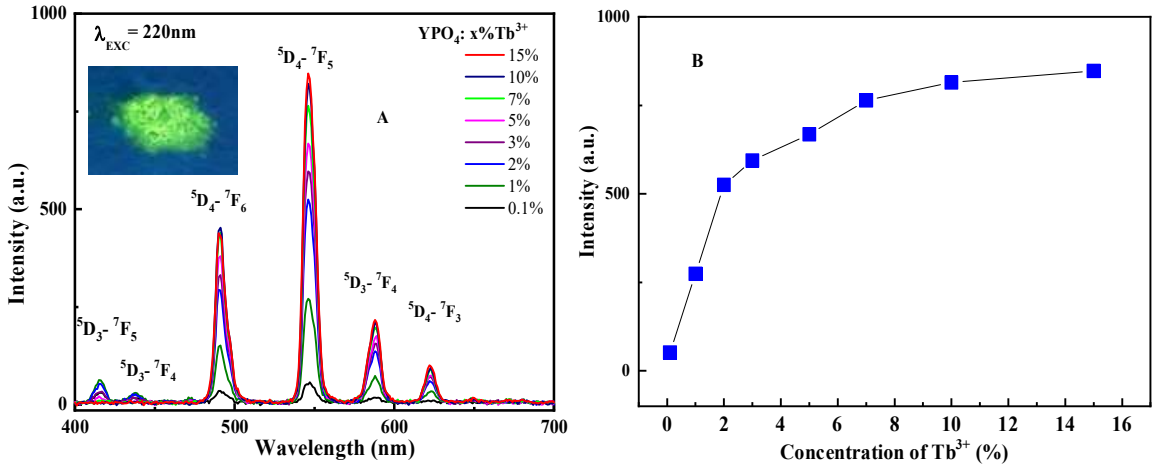

Figure 6. Emission spectra of YPO_4:x%Tb^{3+} samples (A) and the dependence of the intensity of $^5D_4 \rightarrow {}^7F_5$ transition on different concentrations of Tb^{3+} ions (B)

The fluorescence decay curves of YPO_4:x%Tb^{3+} (x = 3, 5, 7, 10, 15) samples for the $^5D_4 \rightarrow {}^7F_5$ transition are presented in the figure. The excitation and emission wavelengths were 220 nm and 550 nm, respectively. It is observed that the emission lifetime of Tb^{3+} ions in all samples followed a single-exponential decay function, described by the equation: $I = I_0 \exp\left(-\frac{t}{\tau}\right)$. where I is the fluorescence intensity at time t, I_0 is the initial intensity, and τ is the luminescence lifetime (Alessandro Esposito, 2008). The measured lifetime values for the material samples are summarized in Table 1.

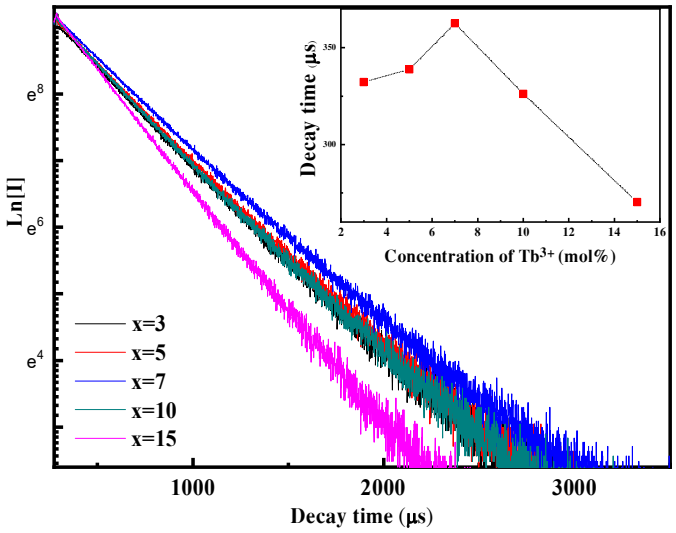

Figure 7. The fluorescence decay curves of YPO_4:x%Tb^{3+}

Table 1. Luminescence decay times of $^5D_4$ (550 nm) in YPO_4:x%Tb^{3+}

Concentration of Tb^{3+}	3 mol%	5 mol%	7 mol%	10 mol%	15 mol%
Decay time (τ) (λ_{ex}=220 nm)(μs)	332	338	363	326	270

For the YPO_4:x%Tb^{3+} material samples, it was observed that the luminescence lifetime increased as the Tb^{3+} concentration increased from 3 mol% to 7 mol%. However, when the concentration exceeded 7 mol%, the lifetime began to decrease. This phenomenon can be explained by the increased interaction between Tb^{3+} ions at higher doping concentrations. As the doping concentration increased, the distance between neighboring Tb^{3+} ions decreased, leading to stronger dipole-dipole interactions. Consequently, in the excited state, non-radiative energy transfer between Tb^{3+} ions became more efficient, which accelerated the depopulation of the excited state and resulted in a shorter luminescence lifetime. This effect highlighted the trade-off between luminescence intensity and lifetime at high doping concentrations, emphasizing 7 mol% Tb^{3+} as the optimal concentration for maintaining a balance between brightness and emission longevity.

4. CONCLUSION

The YPO_4:Tb^{3+} nanomaterial was successfully synthesized using the combustion method, fulfilling the requirements for luminescent nanomaterials research. The synthesized material is single-phase, with an average particle size of 20-30 nm. The optimal calcination temperature under laboratory conditions is 800-900°C. Variations in the Tb^{3+} doping concentration do not significantly affect the material's structure. Under 220 nm excitation, the material exhibits blue emission, with the $^5D_4 \rightarrow {}^7F_5$ transition at 543 nm displaying the highest intensity. The optimal doping concentration in this study is 7 mol%, and the longest measured luminescence lifetime is 363 μs.

References

Alessandro Esposito, Hans C. Gerritsen, Fred S. Wouters, 2008, "Fluorescence

Lifetime Imaging Microscopy: Quality Assessment and Standards", Springer Ser Fluoresc, 6, 117-142.

Bhushan B., *Springer Handbook of Nanotechnology*, 2004, Springer, Berlin, Heidelberg.

Blasse G., B.C. Grabmaier, *Luminescent Materials*, 1994, Springer, Berlin, Heidelberg.

Hemam Jenee Devi, Romeo Singh Loitongbam, W. Rameshwor Singh, 2017, "Luminescence switching in Ce^{3+} ion sensitized YPO_4:Tb^{3+} through Redox reaction", Materials Research Bulletin, 92, pp. 74–84.

Jinyu Yang, Lin Luo, Zhuo Chen, Xueyu Chen, Xiaoyu Tang, 2016, "Tb-doped YPO_4 phosphors: Polyacrylamide gel synthesis and optical properties", Journal of Alloys and Compounds, 689, pp. 837-842.

Junfeng Yang, Xiaoxue Wang, Lina Song, Nan Luo, Jianchao Dong, Shucai GanYang, 2018, "Tunable luminescence and energy transfer properties of $GdPO_4$:Tb^{3+}, Eu^{3+} nanocrystals for warm-white LEDs", Optical Materials, 85, p. 71-78.

Nguyễn Đại Hưng, *Giáo trình huỳnh quang*, 2005, Nhà xuất bản Khoa học và Kỹ thuật Hà Nội.

Phạm Đức Roãn, 2009, *Các nguyên tố hiếm và hóa phóng xạ*, Nhà xuất bản Đại học Sư phạm.

Thái Thị Diệu Hiền, Phạm Đức Roãn, Ngô Khắc Không Minh, Nguyễn Vũ, 2020, "Nghiên cứu tính chất của vật liệu nano phát quang $GdPO_4$:Tb được tổng hợp bằng phản ứng nổ", Tạp chí Khoa học và Công nghệ - Đại học Đà Nẵng, 19(4.2), p. 54-57.

Thái Thị Diệu Hiền, Phạm Đức Roãn, Ngô Khắc Không Minh, Nguyễn Vũ (2021), "Nghiên cứu tính chất của vật liệu nano phát quang YPO_4:Eu được tổng hợp bằng phản ứng nổ", Procedings of Hội nghị Vật lý Chất rắn và Khoa học Vật liệu Toàn quốc – SPMS, 508-511.

Weihua Di, Xiaojun Wang, 2005, "Preparation, characterization and VUV luminescence property of YPO_4:Tb phosphor for a PDP", Optical Materials, 27, p. 1386–1390.

Weihua Di, Xiaojun Wang, Baojiu Chen, Huasheng Lai, Xiaoxia Zhao, "Preparation, characterization and VUV luminescence property of YPO_4:Tb phosphor for a PDP", Optical Materials, 27(8), pp. 1386-1390.

Ying Yu, Lixin Yu, Kangliang Peng, Dandan Sun, Xiaoling Zeng, 2023, "Hydrothermal synthesis and tunable luminescence of YPO_4:Eu^{2+}/Eu^{3+}, Tb^{3+} nanocrystals", Ceramics International, 49(17), pp. 29317-29326.

ẢNH HƯỞNG CỦA NHIỆT ĐỘ TỔNG HỢP, NỒNG ĐỘ ION PHA TẠP ĐẾN TÍNH CHẤT QUANG CỦA VẬT LIỆU NANO YPO_4:Tb^{3+}

TÓM TẮT

Vật liệu nano phát quang YPO_4:Tb^{3+} đã được tổng hợp thành công bằng phương pháp phản ứng nổ. Cấu trúc tinh thể và tính chất quang học được phân tích bằng nhiễu xạ tia X (XRD), quang phổ kích thích huỳnh quang, quang phổ phát xạ và phép đo thời gian sống. Vật liệu tổng hợp là đơn pha với cấu trúc tinh thể tetragonal và kích thước hạt trung bình từ 20 - 30 nm. Dưới ánh sáng kích thích 220 nm, vật liệu cho phát xạ màu xanh lam mạnh tương ứng với các chuyển đổi $^5D_4 \rightarrow {}^7F_J$ của Tb^{3+}, trong đó chuyển dời $^5D_4 \rightarrow {}^7F_5$ là cường độ tốt nhất. Nhiệt độ tổng hợp tối ưu trong điều kiện phòng thí nghiệm là từ 800 đến 900°C, với nồng độ pha tạp Tb^{3+} tốt nhất là 7 mol%. Thời gian sống huỳnh quang đo được của vật liệu là 363 μs.

Từ khóa: *Phản ứng nổ, thời gian sống, vật liệu phát quang, YPO_4:Tb^{3+}*